Am J Physiol Endocrinol Metab 330: E96–E105, 2026.
First published December 5, 2025; doi:10.1152/ajpendo.00061.2025

american physiological society

AMERICAN JOURNAL OF PHYSIOLOGY
ENDOCRINOLOGY AND METABOLISM

RESEARCH ARTICLE

Clinical Metabolism

Intranasal insulin affects brain, but not peripheral tissue, glucose uptake in lean, healthy men: a positron emission tomography study

Aino Latva-Rasku,[1,2] Sanna Laurila,[1,3] Tomi Karjalainen,[1] Riku Klén,[1] Eliisa Löyttyniemi,[4] Olli Eskola,[1] Lauri Nummenmaa,[1,6] Martin Heni,[5] and Pirjo Nuutila[1,2]

[1]*Turku PET Centre, University of Turku, Turku, Finland;* [2]*Department of Endocrinology, Turku University Hospital, Turku, Finland;* [3]*Turku Heart Center, Turku University Hospital, Turku, Finland;* [4]*Department of Biostatistics, University of Turku, Turku, Finland;* [5]*Department of Internal Medicine I, Division of Endocrinology and Diabetology, Ulm University Hospital, Ulm, Germany; and* [6]*Department of Psychology, University of Turku, Turku, Finland*

Abstract

The brain has been suggested to regulate glucose metabolism in response to insulin in various tissues. As many of these findings have not been studied in humans, we aimed to assess the effects of intranasal insulin (INI) on brain and peripheral tissue-specific glucose uptake in lean, healthy men. On two separate visits, 10 volunteers received either 160 IU INI or placebo during a low-dose hyperinsulinemic, euglycemic clamp in a randomized, single-blinded, crossover design. Tissue glucose uptake was quantified using positron emission tomography (PET) and glucose analogue radiotracer 2-deoxy-2[^{18}F]fluoro-D-glucose, with a dynamic scan starting from 40 min after INI. Tissue volumes and radiodensities were assessed with computed tomography. INI induced a global decrease in brain glucose uptake in all participants, with the magnitude of the effect correlating with the amount of visceral adipose tissue. In contrast, INI had no significant effect on skeletal muscle, liver, or adipose tissue glucose uptake. To conclude, a single dose of INI does not have a direct effect on peripheral glucose metabolism in healthy, lean men, but the previously reported hypothalamic response is accompanied by a global decrease in cerebral glucose metabolism.

NEW & NOTEWORTHY In previous studies using functional magnetic resonance imaging, lean, healthy males have been shown to be most susceptible to the effects on intranasal insulin, with direct central insulin exposure also thought to enhance peripheral metabolism. However, in the current study, insulin nasal sprays failed to alter hepatic, skeletal muscle, or adipose tissue glucose metabolism but did induce a global decrease in brain glucose uptake.

insulin sensitivity; intranasal insulin; positron emission tomography; tissue glucose uptake; visceral adipose tissue

INTRODUCTION

In recent years, defective insulin signaling and glucose homeostasis in the central nervous system (CNS) have been associated extensively with metabolic diseases, particularly type 2 diabetes and obesity. Furthermore, brain insulin resistance is linked to neurocognitive decline (1). Details on the role of CNS insulin receptor activation in the regulation of peripheral insulin sensitivity and glucose metabolism have been comprehensively reviewed (2–4).

Studies in rodents have shown that functioning insulin signaling in the medial hypothalamus is crucial for the regulation of both endogenous glucose production (EGP) (5, 6), as well as for white adipose tissue lipolysis and lipogenesis in rodents (7, 8). Although increased whole body glucose consumption after hypothalamic insulin receptor activation is frequently attributed to a significant decrease in EGP with no major effect on other peripheral tissues (6), increased skeletal muscle glycogen synthesis (9) and muscle glucose uptake (10) have also been reported in rodents. However, a study in dogs failed to reproduce the results on central regulation of EGP, showing only a modest suppression of net hepatic glucose output resulting mostly from enhanced glucose uptake and glycogen synthesis (11).

Central effects of insulin have been studied in humans using intranasally administered insulin (INI). When spraying up the nose, insulin reaches the brain via the olfactory nerve tracts, bypassing the blood-brain barrier, as demonstrated in mice (12). The existence of such a direct route in humans has been endorsed by studies that demonstrated rapid changes in cerebrospinal fluid (CSF) insulin concentration (13) and brain activation (14) with only small changes in circulating insulin levels. Using INI, Heni et al. (14, 15) reported increased glucose infusion rates during low-dose hyperinsulinemic, euglycemic

Correspondence: A. Latva-Rasku (aehyyp@utu.fi).
Submitted 5 February 2025 / Revised 27 March 2025 / Accepted 4 November 2025

clamp starting 40–60 min after INI administration in healthy, lean men, as well as a more delayed (190–210 min after INI) increase in glucose rate of disappearance (15). In line with animal studies, INI has been shown to have a suppressing effect on EGP during systemic hyperinsulinemia (15, 16), although the timeframe of the possible effect differs in these two studies, as they used different methods. Despite precipitating hypothalamic activation (14, 15), INI does not seem to influence EGP during fasting (17, 18). Thus, additional direct hepatic insulin action might be necessary for brain-derived effects on liver glucose metabolism (18).

In addition to glucose metabolism, insulin administered to the brain has been shown to reduce lipolysis in mice, possibly via lowered sympathetic nervous system activity in visceral adipose tissue (8). Inhibition of lipolysis by INI has also been suggested by some studies in humans (19); however, this has not been replicated in studies with elevated circulating insulin concentrations (1, 17). Hence, the relevance of these findings for human physiology is still under debate (2).

The current study was aimed at clarifying whether brain insulin action acutely stimulates glucose uptake in lean, healthy men, and if so, which tissues would be affected. We quantified the effects of INI on tissue-specific glucose uptake (GU), primarily in the brain, skeletal muscle, liver, and subcutaneous and brown adipose tissue with positron emission tomography (PET) and a glucose analogue radiotracer 2-deoxy-2-[^{18}F]fluoro-D-glucose ([^{18}F]FDG) together with a low-dose hyperinsulinemic, euglycemic clamp (14, 20). In addition, liver and brown adipose tissue radiodensity were determined from computed tomography (CT) scans to assess tissue fat content. The effect on systemic lipid metabolism was also investigated post hoc from serum samples. We hypothesized that INI could increase GU in peripheral tissues, especially the liver and skeletal muscle, as well as suppress EGP and lipolysis while having no direct effect on brain glucose metabolism.

MATERIALS AND METHODS

Study Participants

Ten healthy, normal weight (BMI 18.5 to 25 kg/m^2), Caucasian male volunteers aged 18–35 yr, not taking any medications, and with normal glucose tolerance based on 75 g oral glucose tolerance test (OGTT), and fasting insulin levels within the hospital reference range were enrolled in the study. Any chronic disease or medication affecting glucose metabolism, history of eating disorders, smoking of tobacco, taking of snuffs or use of narcotics, or significant previous exposure to ionizing radiation led to exclusion from the study. Body fat percentage was measured using bioimpedance [Omron BF400 (MBF-400-E), Omron Healthcare Co. Ltd, Kyoto, Japan].

PET Study Protocol

The study was performed in a randomized, single-blind, crossover design, and all the study visits were performed in Turku PET Center, Turku University Hospital, Turku, Finland. The participants received either 160 IU intranasal insulin or placebo under mild systemic hyperinsulinemia and euglycemia before a whole body [^{18}F]FDG PET scan on two separate study visits 2–16 days apart. The study protocol was approved by the Southwest Finland Hospital District Independent Ethics Committee (ETMK 1/1800/2016). All participants gave written informed consent before any study procedures. The study was registered at ClinicalTrials.gov (Identifier: NCT02933645).

The protocol of scan visits is summarized in Fig. 1. The visits started with the insertion of two venous catheters in opposite forearms, one for infusion of insulin and glucose and injection of [^{18}F]FDG, and another for collection of venous blood samples, arterialized by placing a hot water bottle distally on the arm. After collection of fasting plasma blood samples, a low-dose hyperinsulinemic, euglycemic clamp was started with a bolus of 6.25 mU/kg over 7 min and continued with a dose of 0.25 mU·kg^{-1}·min^{-1} human insulin (Actrapid, Novo Nordisk A/S, Bagsvaerd, Denmark) (14, 20). Euglycemia was maintained with a variable rate infusion of 20% glucose based on plasma glucose measurements performed every 5–10 min.

Nasal insulin sprays were administered 30 min after the start of clamp on both visits as 8 puffs in each nostril over 4 min. To simulate the spillover of insulin into systemic circulation, the participants received an intravenous insulin bolus of 2.5 mU/kg over 15 min together with placebo sprays (15, 18).

Forty minutes after spray application, and 70 min after the start of hyperinsulinemic, euglycemic clamp, the participants were injected with 185 MBq [^{18}F]FDG, manufactured as described earlier (21). The combined PET/CT scan (Discovery 690; General Electric Medical Systems, Milwaukee, WI) was started right after, with dynamic scans of thoracic area (40 min: 4 × 15 s, 6 × 20 s, 2 × 60 s, 2 × 150 s, 6 × 300 s), upper abdomen (15 min: 3 × 300 s), thighs (15 min: 3 × 300 s), and static scans from neck (10 min) and the brain (10 min) scanned sequentially in the same session, and with the clamp continuing until the end of scan, a total of 160 min. Amount of [^{18}F]FDG lost into urine was measured from a urine sample given at the end of scan using an isotope dose calibrator (Model VDC-205, Comecer Netherlands, Joure, the Netherlands).

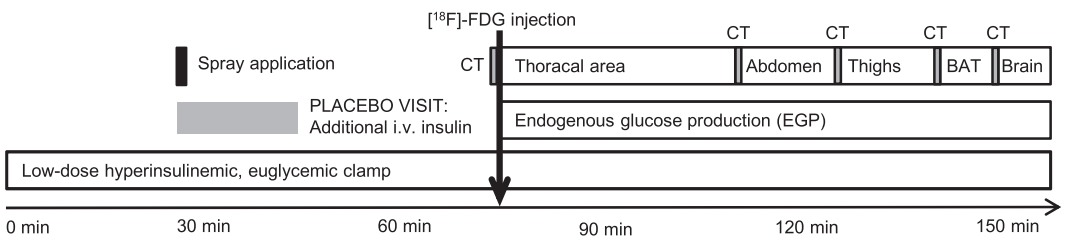

Figure 1. Study protocol on visits with PET scans. PET, positron emission tomography.

Nasal Insulin and Placebo Sprays

Spray bottles containing either intranasal insulin (100 IU/mL, Actrapid, Novo Nordisk A/S, Bagsvaerd, Denmark) or placebo (Insulin Diluting Medium for NovoRapid and Levemir, Novo Nordisk A/S, Bagsvaerd, Denmark) were manufactured by the local hospital pharmacy. The sprays were administered to the participants in a single-blinded fashion, with the order randomized in blocks.

PET Data Analysis

Before analysis, all PET data were corrected for dead time, decay, and photon attenuation. Input function was obtained by combining activity data from PET images from inside the left ventricle, and plasma samples collected at nine time points during the scan, and analyzed with an automated gamma counter (Wizard 1480 3, Wallac, Turku, Finland). Tissue activity was determined using Carimas software (Version 2.9, Turku PET Centre, http://www.turkupetcentre.fi), applying free-hand drawn region of interests for other tissues: both quadriceps femoris muscles, right lobe of the liver, supraclavicular brown adipose tissue depots, and several smaller volumes of abdominal subcutaneous adipose tissue. The acquired time-activity curves from different tissues and blood were then compared with determine radiotracer uptake using the Patlak-Gjedde plot (K_i) (22) or its estimate, fractional uptake rate (FUR) (23).

Next, tissue GU ($\mu mol \cdot kg^{-1} \cdot min^{-1}$) was calculated by multiplying K_i or FUR with plasma glucose level, and dividing by tissue density and a constant accounting the differences in metabolic rates of [^{18}F]FDG and glucose [1.2 for skeletal muscle (24), 1.0 for liver (25), 1.14 for adipose tissue (26), 0.65 for the brain (27)].

Glucose uptake in the brain was obtained using SPM12-based toolbox Magia (28), with GU calculated from FUR results. The data were then spatially normalized to Montreal Neurological Institute (MNI) space using an in-house [^{18}F]FDG template and finally smoothed with a Gaussian kernel with 8-mm full-width at half-maximum.

EGP was assessed by subtracting the amount of glucose infused after injection from the whole body glucose disappearance rate (R_d) derived from [^{18}F]FDG consumption (29).

Visceral Adipose Tissue Area

Visceral adipose tissue area was measured from a single cross-sectional CT image below and adjacent to the left kidney on the insulin spray visit by using sliceOmatic (v.5.0, TomoVision, Canada). The area includes both intra- and retroperitoneal fat deposits.

Tissue Radiodensity

Tissue radiodensity was used as a proxy of tissue fat content, with lower values indicating higher adiposity. Regions of interest were manually drawn on the CT images using Carimas Software. In the liver, a spherical volume of interest (VOI) was drawn on the right lobe using the same anatomical area on both visits. Brown adipose tissue (BAT) VOIs were drawn on the supraclavicular fat depots and visceral adipose tissue VOIs in retroperitoneal adipose tissue, including only voxels with CT Hounsfield units (HU) within the adipose tissue range (−50 to −250) (30).

Serum Metabolites

Serum samples were collected from the first nine participants and used for comprehensive analysis of metabolites at Nightingale Health Ltd laboratory, using nuclear magnetic resonance (31), with the focus on serum total fatty acids, glycerol, triacylglycerols (TAGs) in VLDL, LDL, and HDL as well as total serum TAGs, and apolipoproteins A-I and B. Samples were collected at fasting, during clamp before nasal spray administration, as well as 60 and 90 min after administration.

Statistical Analyses

The sample size was determined to detect a 22% placebo-corrected change in glucose infusion rate, based on unpublished results from Tübingen, with 95% power at a two-tailed significance level of 5%. Analyses were performed using a mixed model for repeated measurements with fixed effects of intervention, period, and sequence (=intervention order). The results are reported as INI-induced mean changes compared with placebo with a 95% confidence interval (CI). Changes in brain GU were estimated using a paired *t*-test in SPM12, with $P < 0.05$ as the cluster-defining threshold. Only statistically significant clusters ($P < 0.05$, family-wise error rate (FWE)-corrected) are reported. Associations were studied with Pearson correlation. For serum metabolites, changes from spray application to 60 and 90 min later were compared between interventions using a paired Wilcoxon signed-rank test with RStudio (RStudio Inc., Boston, MA).

RESULTS

Participant Characteristics

Baseline measurements made on the screening visit are presented in Table 1. One participant was excluded from BAT analysis due to abnormally high activation of the tissue on the placebo visit, but otherwise, the whole data set was used in the analyses.

INI Effects on Plasma Glucose and Insulin during Clamp

Plasma glucose values were comparable and within euglycemia during both interventions (Fig. 2*A*). Despite the additional intravenous insulin administered with the placebo sprays, serum insulin levels were numerically higher after INI from 25 min after the sprays until the end of study

Table 1. *Participant characteristics*

	Whole Group (n = 10)	
	Mean	Range
Age, yr	24	20–28
Weight, kg	76.8	65.2–87.5
BMI, kg/m^2	23.5	20–25.6
Fat percentage, %	16.5	9.7–20.3
Waist-to-hip ratio	0.84	0.80–0.91
Fasting plasma glucose, mmol/L	5.2	3.7–5.8
HbA1c, mmol/mol	29	24–32
HbA1c, %	4.8	4.3–5.1
Fasting plasma insulin, pmol/L	35	7–69
HOMA-IR	1.33	0.16–2.40
Matsuda-ISI	9.4	3–27.2

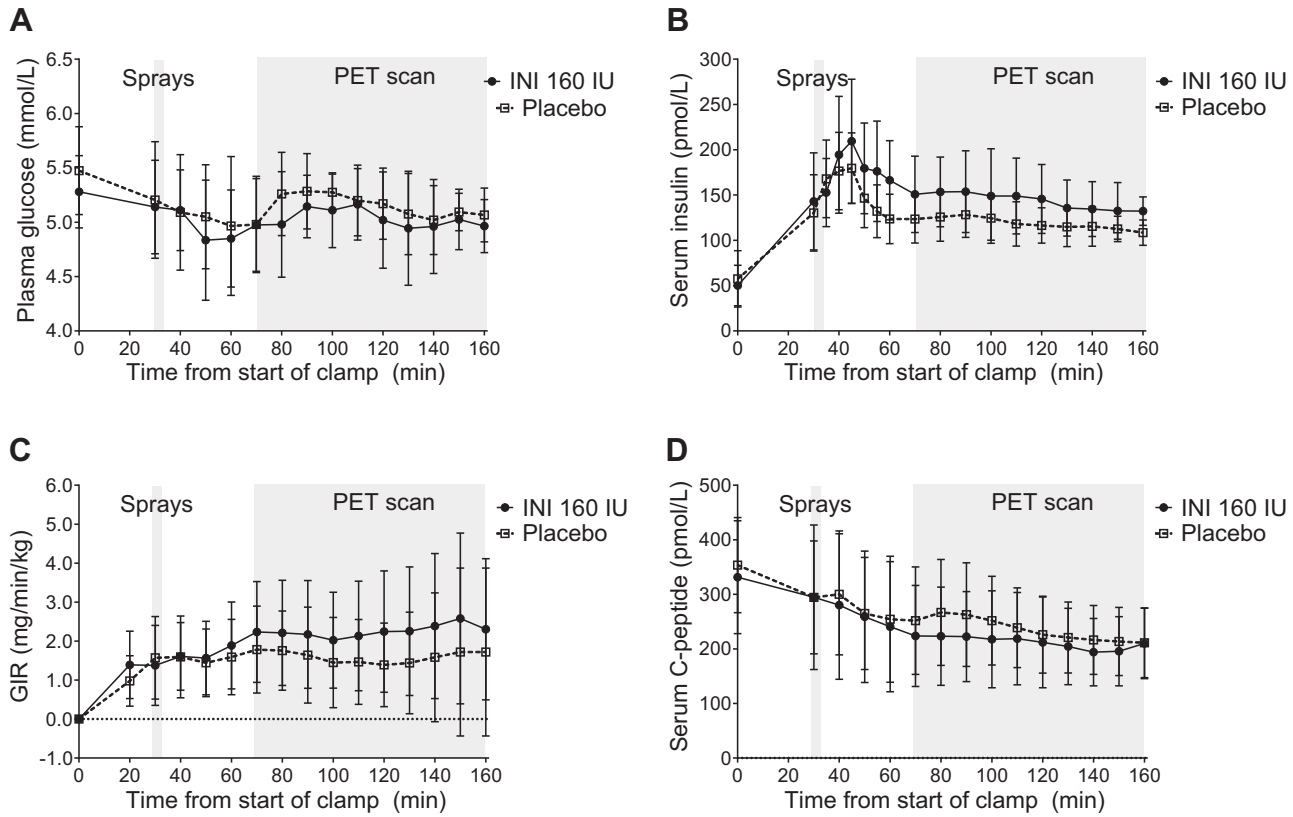

Figure 2. Plasma glucose (mmol/L) (*A*); serum insulin (pmol/L) (*B*) and C-peptide (pmol/L) concentrations (*D*) during the studies. *C*: glucose infusion rate (GIR, mg·kg^{-1}·min^{-1}) during the studies. Data are mean and SD. The gray background represents the 4-min period of spray application at 30 min, and the PET scan periods. PET, positron emission tomography.

(Fig. 2*B*). However, the difference in mean insulin levels after spray application did not reach statistical significance (19.4 pmol·L^{-1}, 95% CI −2.0, 40.8, $P = 0.07$), and the degree of change in insulin levels did not correlate with tissue GU or radiodensity results. Serum C-peptide levels were numerically lower after INI, but the difference to placebo was not statistically significant (at the time of maximal difference at 80 min, the mean difference was 43.6 nmol·L^{-1}, 95% CI −95.4, 8.2, $P = 0.09$). In addition, no significant treatment effects were observed in serum lactate ($P = 0.90$), β-hydroxybutyrate ($P = 0.22$), or acetoacetate ($P = 0.40$).

Suppressed Brain GU after INI

GU to the brain was globally lower after INI administration, with the hypothalamus and more anterior brain regions showing a slightly stronger treatment effect (Fig. 3, Fig. 5*B*, and Table 2).

Both the glucose uptake rate after INI and the difference in GU between interventions correlated with visceral adipose tissue area (Fig. 4), whereas the associations were not evident after placebo, and there was no correlation with brain GU and body fat percentage on either of the visits (P values > 0.40). The associations were strongest in cortical areas and regions involved with memory, in comparison to deeper brain structures (Supplemental Table S1). OGTT-derived Matsuda insulin sensitivity index or HOMA-IR showed no significant correlations with the change in brain GU ($r = -0.48$, $P = 0.16$, and $r = 0.42$, $P = 0.23$, respectively). After placebo, brain GU correlated significantly with [^{18}F]FDG R_d ($r = -0.67$, $P =$

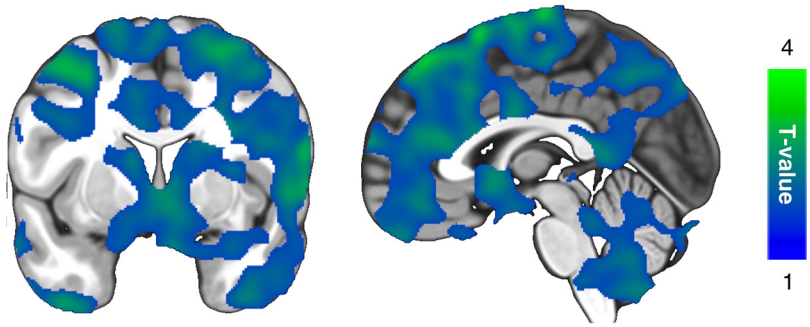

Figure 3. Compared with placebo, INI lowered brain GU globally, with the higher *T*-value (green) indicating areas of strongest decrease in GU. The data are thresholded at $P <$ 0.05 and FWE-corrected at cluster level. The *x* and *y* coordinates in the frontal (*left*) and sagittal (*right*) planes refer to the neuroanatomical locations of the slices in the MNI space. GU, glucose uptake; INI, intranasal insulin; MNI, Montreal Neurological Institute.

Table 2. *Mean brain glucose uptake rates (μmol/100 g/min) in different anatomical and functional regions, confidence interval for the change from placebo to post intranasal insulin sprays, and the respective P values for the change*

	INI	Placebo		
	Mean (SD)	Mean (SD)	95 % CI	*P* Value
Whole brain	21.5 (2)	21.7 (1)	−1.8, 0.2	0.09
Grey matter	23.7 (2.1)	23.9 (1.1)	−2.0, 0.2	0.09
White matter	17.9 (1.7)	18.0 (1)	−1.5, 0.2	0.10
Cerebellum	19.4 (1.6)	19.6 (0.8)	−2.0, 0.2	0.11
Frontal lobe	22.9 (2.2)	23.0 (1.2)	−1.9, 0.1	0.07
Frontotemporal region	21.2 (2.4)	21.4 (1.2)	−1.9, 0.2	0.10
Limbic lobe	21.4 (1.9)	21.5 (1)	−1.8, 0.1	0.08
Medulla	16.1 (1.5)	16.5 (0.8)	−1.9, 0.2	0.10
Midbrain	18 (1.5)	18.3 (1)	−1.9, 0.3	0.13
Occipital lobe	22.4 (2)	22.6 (1.1)	−2.0, 0.3	0.14
Parietal lobe	24.3 (2.2)	24.4 (1.2)	−1.9, 0.2	0.08
Pons	13.8 (1.2)	14.0 (0.6)	−1.5, 0.3	0.14
Temporal lobe	21.2 (1.8)	21.2 (1)	−1.5, 0.2	0.11
Dorsal attention network	23.7 (2.2)	23.8 (1.2)	−1.8, 0.1	0.08
Frontoparietal region	26.3 (2.7)	26.5 (1.5)	−2.2, 0.2	0.08
Somatomotor cortex	23.2 (2)	23.3 (1.1)	−1.8, 0.1	0.08
Ventral attention network	24.2 (2.3)	24.4 (1.2)	−1.9, 0.2	0.08
Visual cortex	21.6 (1.9)	21.8 (1)	−1.8, 0.2	0.11
Inferior temporal gyrus	23.2 (2)	23.3 (1.1)	−1.8, 0.2	0.10
Posterior cingulate cortex	26.9 (2.3)	27.1 (1.2)	−2.3, 0.3	0.10
Angular gyri	23.5 (2.4)	23.6 (1.4)	−1.9, 0.2	0.10
Hypothalamus	13.9 (1.5)	14.6 (1.4)	−1.3, −0.2	0.015

CI, confidence interval; INI, intranasal insulin.

0.03) and skeletal muscle GU ($r = -0.72$, $P = 0.02$), whereas the associations were not statistically significant after INI ($r = -0.56$, $P = 0.09$ and $r = -0.49$, $P = 0.15$, respectively). EGP did not correlate with brain GU on either visit ($P > 0.67$).

No Effect on Whole Body or Skeletal Muscle GU

Glucose infusion rates (GIRs) were not significantly affected by INI (Fig. 2*C*) (at the time of maximal difference at 120 min, 0.9 mg·kg^{-1}·min^{-1}, 95% CI −0.2, 1.9, $P = 0.09$). Furthermore, rate of total radiotracer-derived glucose disappearance (R_d) during the scan was not significantly altered by INI (Fig. 5*A*, 2.4 μmol·kg^{-1}·min^{-1}, 95% CI −1.3, 6.1, $P = 0.17$). In line with this, skeletal muscle GU was not affected by INI (Fig. 5*A*, mean change 0.3 μmol·kg^{-1}·min^{-1}, 95% CI −1.8, 2.5, $P = 0.75$).

Increased Tissue Radiodensity in the Liver, but no Change in Glucose Uptake or Output

INI did not increase GU into liver (Fig. 5*A*, 1.0 μmol·kg^{-1}·min^{-1}, 95% CI −1.6, 3.7, $P = 0.39$) or affect EGP (−2.5 μmol·kg^{-1}·min^{-1}, 95% CI −6.3, 1.2, $P = 0.16$). Hepatic tissue radiodensity was significantly higher after INI ($P = 0.03$), and the difference in tissue density correlated positively with the difference in plasma insulin levels during the scan ($r = 0.73$, $P = 0.03$).

Unaffected Adipose Tissue GU, Decreased BAT Radiodensity

There was no significant changes in waist subcutaneous adipose tissue (0.2 μmol·kg^{-1}·min^{-1}, 95% CI −1.5, 1.9, $P = 0.79$), visceral adipose tissue (1.9 μmol·kg^{-1}·min^{-1}, 95% CI −2.2, 6.2, $P = 0.32$), or BAT GU (−1.09 μmol·kg^{-1}·min^{-1}, 95% CI −13.4, 11.2, $P = 0.83$) in response to INI (Fig. 5*A*). In brown adipose tissue radiodensity was lower after INI (−1.4 HU, 95% CI −2.5, −0.3, $P = 0.02$), whereas it was similar in visceral adipose tissue (−0.3 HU, −95% CI 3.4, 2.8, $P = 0.84$).

Serum Lipids

Levels of serum total fatty acids, glycerol, TAGs in VLDL, LDL, and HDL, total TAGs, or apolipoproteins A-I and B were not significantly affected by INI in the whole group or when looking at the subgroups separately. The results are detailed in Supplemental Figs. S1 and S2.

DISCUSSION

Our study shows that a single intranasal dose of insulin affects brain glucose uptake measured with [^{18}F]FDG-PET under mild systemic hyperinsulinemia without affecting peripheral glucose uptake in lean, healthy men. Similarly, lipolysis or TAG production was not altered to a degree measurable in serum concentrations of different metabolites.

To date, investigations into the effects of intranasal insulin on cerebral glucose uptake in humans have been limited, with most research focusing on INIs functional and peripheral metabolic effects rather than its impact on the metabolism of the brain itself. However, our findings align with previous research demonstrating a global decrease in brain glucose uptake following intranasal insulin administration during fasting in healthy mice (32). Also, the stronger regional effect

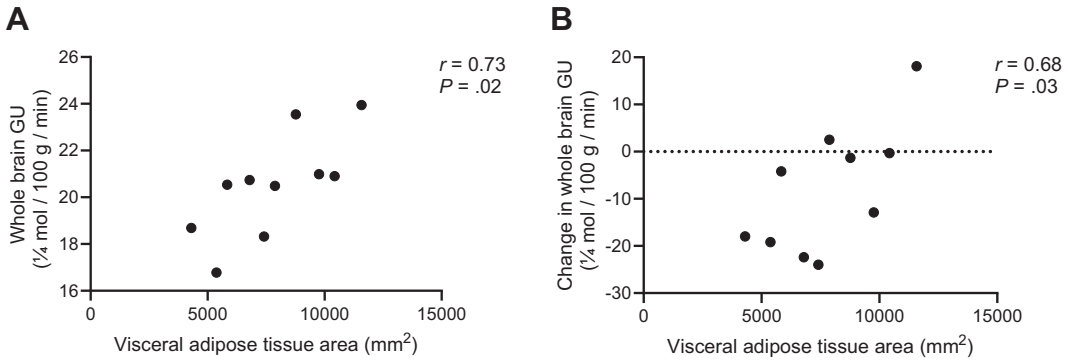

Figure 4. Smaller amount of visceral adipose tissue correlated with a decreased need for glucose after INI, as seen both in glucose uptake (GU) after INI (*A*), and when comparing the difference in GU after INI vs. placebo (*B*). INI, intranasal insulin.

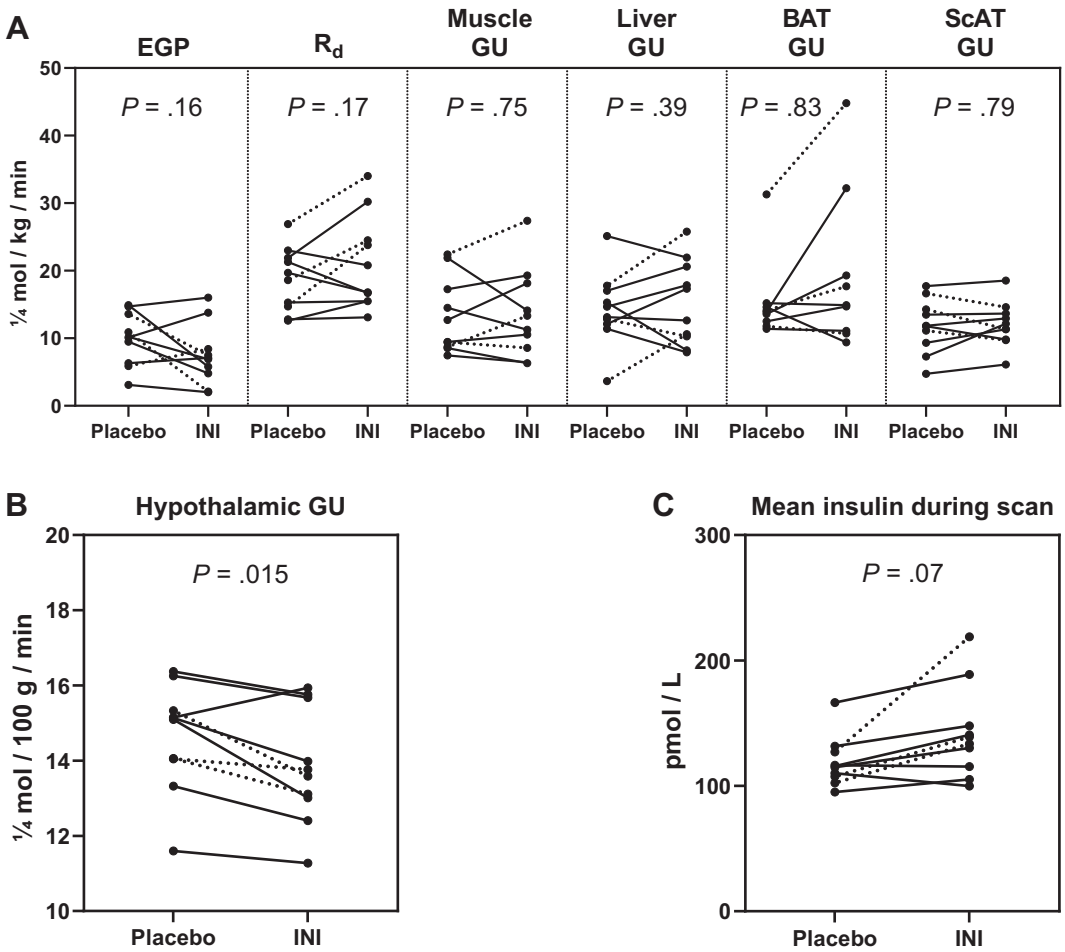

Figure 5. *A*: There were no significant differences in endogenous glucose production (EGP), rate of [^{18}F]FDG disappearance (R_d), or glucose uptake (GU) into skeletal muscle, liver, brown adipose tissue (BAT) or subcutaneous adipose tissue (ScAT) after INI or placebo. *B*: After INI, hypothalamic GU was significantly lower than after placebo. Although mean insulin levels were not statistically significantly different between visits (*C*), the three subjects with numerically higher serum insulin levels are identified with dashed lines in all graphs. INI, intranasal insulin.

on the hypothalamus and anterior brain areas align with rodent studies using radioligand-labelled insulin (33).

Previously, increasing plasma insulin levels during hyperinsulinemic, euglycemic clamp has been shown to increase brain glucose uptake by 3%–4% compared with fasted state in healthy participants (34), or up to 15% while suppressing endogenous insulin secretion with somatostatin (35). Therefore, the 3.3%–5.1% decrease seen in the current study is likely dependent on the route of insulin administration, as well as the timing of [^{18}F]FDG injection, and may be attributed to several factors.

For one, insulin reaches the central nervous system (CNS) within 10–40 min postadministration (13), potentially inducing widespread neuronal activation initially, leading to increased glycolysis (36). Subsequently, during the recovery phase, lactate produced by glial cells may become the preferred fuel source (36), in the expense of glucose and [^{18}F]FDG. Moreover, it has been shown that brain glycogen content decreases within 15 min of activation and slowly recovers within the next hour, indicating that glycogenolysis might also serve as another source for glucose or lactate during the recovery period (37). Interestingly, a similar decrease in brain [^{18}F]FDG uptake has been observed following oral glucose administration (23).

Alternatively, it cannot be excluded that the effects of intranasal insulin on brain glucose uptake may result from direct modulation of cellular insulin-mediated glucose metabolism. Despite brain glucose metabolism not being dependent on insulin, insulin has been shown to increase GLUT4 transportation to the plasma membrane in neurons and stimulate GU in vitro (38) and in mice (39), and to promote glycogen synthesis, but not GU, in astrocytes in vitro (40). From a methodological standpoint, we cannot exclude the possibility that increased efflux of glucose from brain tissue to the circulation occurred following INI (41), as we were unable to perform extended dynamic brain imaging to more comprehensively characterize [^{18}F]FDG kinetics. However, even if an increased tracer washout was present, it could be argued that such an effect reflects a reduced cerebral glucose demand following INI, although the underlying mechanism remains uncertain.

Although the exact cellular mechanisms underlying the observed decrease in brain glucose uptake remain elusive, our findings are consistent with previous reports. Intriguingly, INI has been shown to reduce appetite and food intake (2), whereas increasing brain ATP and phosphocreatine levels shortly after administration (42), suggesting a potential link

between decreased glucose uptake and the anorexigenic effects of intranasal insulin.

Previous studies have linked higher volumes of visceral adipose tissue to impaired hypothalamic response to insulin and altered brain glucose metabolism during systemic hyperinsulinemia (43, 44). Interestingly, visceral adiposity seems to be a more significant determinant of brain insulin responsiveness than peripheral insulin sensitivity or whole body fat percentage measured with bioimpedance, as evidenced also by our results, showing diminished metabolic effects of INI in subjects with a higher amount of visceral adipose tissue. Moreover, the differences were more pronounced in brain regions involved with cognition and memory. Our findings do not support the notion of an acute central regulation of visceral adipose tissue metabolism, as glucose uptake and tissue radiodensity did not differ between interventions. Although the detrimental effects of excess visceral adiposity on brain health are well-established (45), the mechanisms underlying potential brain control of visceral adipose tissue metabolism remain under investigation, with lacking data in humans (46).

We did not observe changes in peripheral tissue glucose uptake, with rates of GU and EGP resembling fasting rather than insulin-stimulated levels, despite the slightly higher circulating insulin levels after INI. Currently, only one study in mice has reported increased directly measured GU in skeletal muscle during clamp conditions, with no effect observed in other peripheral tissues (10), while other studies report no effect in any peripheral tissue (8). Moreover, we did not observe a significant increase in GIR toward the end of the study, suggesting that relevant later effects within 120 min from spray application are unlikely, consistent with previous findings that central ATP-sensitive potassium (K_{ATP}) channel activation significantly suppresses EGP without affecting glucose disappearance rate or GIR after 6 h of administration during pancreatic clamp (47). Therefore, it appears that the previously reported effects of INI on whole body glucose disposal primarily occur in the presence of increased circulating insulin levels, although suppression of EGP at a later time point is also possible.

The method used to measure EGP in the current study only provides an average over the entire duration of the scan (approximately 40–120 min post sprays). Consequently, the absence of change in EGP in our current study does not contradict prior research combining INI and systemic insulin administration, as these earlier studies documented decreases in EGP 100–120 min or 3 to 6 h after administration of human insulin (15) or an insulin analogue (16). Thus, our findings remain consistent with this existing body of literature but indicate that brain-derived effects on EGP might be of transient nature.

The observed increase in liver radiodensity, a proxy of tissue lipid content, aligns with what Gancheva et al. (17) have reported earlier. Although it cannot be excluded that the brain may regulate hepatic lipid turnover, the strong correlation between higher liver radiodensity and higher plasma insulin levels after INI in the current study suggests that central regulation is likely secondary to direct effects of insulin (11). As Gancheva et al. (17) also hypothesized, the transient decrease in hepatic lipid content can also be secondary to the inhibition of lipolysis in adipose tissue by circulating insulin.

Opposite to the liver, INI decreased tissue radiodensity in supraclavicular BAT, likely indicating inhibition of lipolysis in the tissue. Interestingly, we did not observe a change in glucose uptake rate, whereas intravenous insulin administration has been reported to induce a fivefold increase in uptake (48). Although direct effects of insulin on BAT can also explain the result, it is possible that BAT lipolysis and lipogenesis are, in part, centrally regulated, as previously shown in white adipose tissue in mice (8). As BAT activation is typically associated with consumption of BAT triglycerides and an increase in radiodensity (30), INI did not appear to activate BAT in our study. Preclinical studies suggest that intracerebroventricular administration of insulin induces BAT thermogenesis, but this effect seems to depend on the dose of insulin and feeding status (49), supporting the hypothesis of the gut being an important independent regulator of BAT activity. Notably, in humans, INI has been shown to enhance thermogenesis in the postprandial state (50), whereas our study was conducted under fasting conditions.

In mice, decreased lipolysis and lipogenesis following insulin administration to the mediobasal hypothalamus led to a decrease in the rate of appearance of glycerol (8). Transient lowering of glycerol appearance has also been reported in humans 0–60 min after INI administration during fasting (19), whereas glycerol levels in circulation and subcutaneous white adipose tissue interstitium remained unchanged (17, 19). Similarly, we observed no significant changes in serum glycerol. Furthermore, there were no changes in serum TAGs, apolipoproteins, or total fatty acids, consistent with previous studies during fasting (17, 19) and pancreatic clamp (51). The relevance of brain-derived signals on lipolysis compared with direct effects of insulin on white adipocytes under physiological circumstances remains under discussion (2), and our results argue against a major contribution.

Although the strengths of this study are the established methods and site experience in measuring tissue GU quantitatively using PET, the approach also has limitations. The assessment of tissue GU is confined to the moment of injection, after which most of the radiotracer available is trapped within cells during the initial 20 min, focusing this study primarily on the effects observed 40–60 min after INI administration. However, our protocol closely aligns with earlier reports on insulin transportation speed and action. Notably, the increase in cerebrospinal fluid (CSF) insulin concentration begins within 10 min (13), hypothalamic activation can be seen at 30 min, and an increase in GIR should commence 40 min after INI administration (14).

In comparison to previous studies, our participants had higher body mass index (BMI), and it has been demonstrated that the effects of INI on hypothalamic activation appear to diminish in people with overweight or obesity (14, 52). However, the participants with higher BMI were mostly also more insulin sensitive, likely due to higher muscle mass, as they also had less visceral adipose tissue. Finally, the small sample size and inclusion of only male participants limits the generalizability of the results, as females have been shown to respond differently to the appetite-suppressing effect of INI and also demonstrate different fMRI responses (53). Considering the small sample size, variability of insulin response depending on menstrual cycle phase (54), and the

more strict local radiation safety precautions in women of fertile age, the choice to include only male participants can, however, be considered justified.

To conclude, we observed no change in peripheral tissue or whole body glucose metabolism in response to INI during the first 40–120 min after administration. Tissue radiodensity increased in the liver after INI, whereas lipolysis was inhibited in brown adipose tissue, but whether these changes are centrally regulated or elicited by direct effects of insulin remains to be determined.

However, we found that 40 min after INI administration, brain glucose uptake is significantly reduced, possibly due to energy needs being met by alternative fuel sources. Importantly, brain metabolic response was attenuated by higher visceral adiposity even in normal-weight, insulin-sensitive, young men, consistent with previous reports from functional brain imaging studies. These findings emphasize the cross talk between visceral adipose tissue and the brain, especially in the early phases of central insulin resistance.

Finally, while insulin has been suggested to modulate a range of processes via direct effects on the brain, including appetite regulation, peripheral glucose homeostasis, cognitive functions such as learning and memory, reward processing, and mood, the findings in humans remain conflicting, partly due to different approaches in how brain insulin sensitivity or resistance is measured and defined. Given the complexity of brain insulin action, a single diagnostic modality is unlikely to capture its dysfunction comprehensively, and further studies combining different approaches are warranted to further characterize insulin resistance and insulin action in the CNS.

DATA AVAILABILITY

The data that support the findings of this study are available from the corresponding author, [A.L.-R.], upon reasonable request.

SUPPLEMENTAL MATERIAL

Supplemental Table S1 and Supplemental Figs. S1 and S2: https://doi.org/10.6084/m9.figshare.30182416.

ACKNOWLEDGMENTS

We thank the study volunteers for their participation, and study nurse Mia Koutu for work in the study. The authors also thank Aero Pump GmbH, Hochheim/Main, Germany for kindly providing the nasal pumps used in the study.

Present addresses: A. Latva-Rasku, Turku PET Center, University of Turku, Turku, Finland and Department of Endocrinology, Turku University Hospital, Turku, Finland; S. Laurila, Turku Heart Center, Turku University Hospital, Turku, Finland; T. Karjalainen, Data Craftery Oy, Oulu, Finland; R. Klén, Turku PET Centre, University of Turku, Turku, Finland; E. Löyttyniemi, Department of Biostatistics, University of Turku, Turku, Finland; O. Eskola, Turku PET Centre, University of Turku, Turku, Finland; L. Nummenmaa, Turku PET Center, University of Turku, Turku, Finland and Department of Psychology, University of Turku, Finland; M. Heni, Department of Internal Medicine I, Division of Endocrinology and Diabetology, Ulm University Hospital, Ulm, Germany; P. Nuutila, Turku PET Centre, University of Turku, Turku, Finland and Department of Endocrinology, Turku University Hospital, Turku, Finland.

GRANTS

The study was conducted within the Finnish Center of Excellence in Molecular Imaging in Cardiovascular and Metabolic Research supported by the Academy of Finland. The work was supported by personal grants from The Finnish Diabetes Research Foundation, Finnish Cultural Foundation Varsinais-Suomi Regional Fund, and Sakari Alhopuro Foundation (to A.L.-R.).

DISCLOSURES

No conflicts of interest, financial or otherwise, are declared by the authors.

AUTHOR CONTRIBUTIONS

A.L.-R., S.L., M.H., and P.N. conceived and designed research; A.L.-R., S.L., T.K., and O.E. performed experiments; A.L.-R., S.L., T.K., R.K., E.L., and L.N. analyzed data; A.L.-R., S.L., T.K., R.K., L.N., and M.H. interpreted results of experiments; A.L.-R., T.K., R.K., and L.N. prepared figures; A.L.-R. drafted manuscript; A.L.-R., S.L., T.K., R.K., E.L., O.E., L.N., M.H., and P.N. edited and revised manuscript; A.L.-R., S.L., T.K., R.K., E.L., O.E., L.N., M.H., and P.N. approved final version of manuscript.

REFERENCES

1. **Kellar D**, **Craft S.** Brain insulin resistance in Alzheimer's disease and related disorders: mechanisms and therapeutic approaches. *Lancet Neurol* 19: 758–766, 2020. doi:10.1016/S1474-4422(20)30231-3.
2. **Kullmann S**, **Kleinridders A**, **Small DM**, **Fritsche A**, **Häring HU**, **Preissl H**, **Heni M.** Central nervous pathways of insulin action in the control of metabolism and food intake. *Lancet Diabetes Endocrinol* 8: 524–534, 2020. doi:10.1016/S2213-8587(20)30113-3.
3. **Scherer T**, **Sakamoto K**, **Buettner C.** Brain insulin signalling in metabolic homeostasis and disease. *Nat Rev Endocrinol* 17: 468–483, 2021. doi:10.1038/S41574-021-00498-X.
4. **Heni M.** The insulin resistant brain: impact on whole-body metabolism and body fat distribution. *Diabetologia* 67: 1181–1191, 2024. doi:10.1007/s00125-024-06104-9.
5. **Obici S**, **Zhang BB**, **Karkanias G**, **Rossetti L.** Hypothalamic insulin signaling is required for inhibition of glucose production. *Nat Med* 8: 1376–1382, 2002. doi:10.1038/NM1202-798.
6. **Pocal A**, **Lam TKT**, **Gutierrez-Juarez R**, **Obici S**, **Schwartz GJ**, **Bryan J**, **Aguilar-Bryan L**, **Rossetti L.** Hypothalamic K(ATP) channels control hepatic glucose production. *Nature* 434: 1026–1031, 2005. doi:10.1038/NATURE03439.
7. **Koch L**, **Wunderlich FT**, **Seibler J**, **Könner AC**, **Hampel B**, **Irlenbusch S**, **Brabant G**, **Kahn CR**, **Schwenk F**, **Brüning JC.** Central insulin action regulates peripheral glucose and fat metabolism in mice. *J Clin Invest* 118: 2132–2147, 2008. doi:10.1172/JCI31073.
8. **Scherer T**, **O'Hare J**, **Diggs-Andrews K**, **Schweiger M**, **Cheng B**, **Lindtner C**, **Zielinski E**, **Vempati P**, **Su K**, **Dighe S**, **Milsom T**, **Puchowicz M**, **Scheja L**, **Zechner R**, **Fisher SJ**, **Previs SF**, **Buettner C.** Brain insulin controls adipose tissue lipolysis and lipogenesis. *Cell Metab* 13: 183–194, 2011. doi:10.1016/J.CMET.2011.01.008.
9. **Perrin C**, **Knauf C**, **Burcelin R.** Intracerebroventricular infusion of glucose, insulin, and the adenosine monophosphate-activated kinase activator, 5-aminoimidazole-4-carboxamide-1-beta-D-ribofuranoside, controls muscle glycogen synthesis. *Endocrinology* 145: 4025–4033, 2004. doi:10.1210/EN.2004-0270.
10. **Coomans CP**, **Biermasz NR**, **Geerling JJ**, **Guigas B**, **Rensen PCN**, **Havekes LM**, **Romijn JA.** Stimulatory effect of insulin on glucose uptake by muscle involves the central nervous system in insulin-sensitive mice. *Diabetes* 60: 3132–3140, 2011. doi:10.2337/DB10-1100.
11. **Ramnanan CJ**, **Saraswathi V**, **Smith MS**, **Donahue EP**, **Farmer B**, **Farmer TD**, **Neal D**, **Williams PE**, **Lautz M**, **Mari A**, **Cherrington AD**, **Edgerton DS.** Brain insulin action augments hepatic glycogen synthesis without suppressing glucose production or gluconeogenesis in dogs. *J Clin Invest* 121: 3713–3723, 2011. doi:10.1172/JCI45472.

12. **Renner DB**, **Svitak AL**, **Gallus NJ**, **Ericson ME**, **Frey WH**, **Hanson LR.** Intranasal delivery of insulin via the olfactory nerve pathway. *J Pharm Pharmacol* 64: 1709–1714, 2012. doi:10.1111/J.2042-7158.2012.01555.X.
13. **Born J**, **Lange T**, **Kern W**, **McGregor GP**, **Bickel U**, **Fehm HL.** Sniffing neuropeptides: a transnasal approach to the human brain. *Nat Neurosci* 5: 514–516, 2002. doi:10.1038/NN849.
14. **Heni M**, **Wagner R**, **Kullmann S**, **Veit R**, **Mat Husin H**, **Linder K**, **Benkendorff C**, **Peter A**, **Stefan N**, **Häring HU**, **Preissl H**, **Fritsche A.** Central insulin administration improves whole-body insulin sensitivity via hypothalamus and parasympathetic outputs in men. *Diabetes* 63: 4083–4088, 2014. doi:10.2337/db14-0477.
15. **Heni M**, **Wagner R**, **Kullmann S**, **Gancheva S**, **Roden M**, **Peter A**, **Stefan N**, **Preissl H**, **Häring HU**, **Fritsche A.** Hypothalamic and striatal insulin action suppresses endogenous glucose production and may stimulate glucose uptake during hyperinsulinemia in lean but not in overweight men. *Diabetes* 66: 1797–1806, 2017. doi:10.2337/DB16-1380.
16. **Dash S**, **Xiao C**, **Morgantini C**, **Koulajian K**, **Lewis GF.** Intranasal insulin suppresses endogenous glucose production in humans compared with placebo in the presence of similar venous insulin concentrations. *Diabetes* 64: 766–774, 2015. doi:10.2337/DB14-0685.
17. **Gancheva S**, **Koliaki C**, **Bierwagen A**, **Nowotny P**, **Heni M**, **Fritsche A**, **Häring HU**, **Szendroedi J**, **Roden M.** Effects of intranasal insulin on hepatic fat accumulation and energy metabolism in humans. *Diabetes* 64: 1966–1975, 2015. doi:10.2337/db14-0892.
18. **Plomgaard P**, **Hansen JS**, **Ingerslev B**, **Clemmesen JO**, **Secher NH**, **van Hall G**, **Fritsche A**, **Weigert C**, **Lehmann R**, **Häring HU**, **Heni M.** Nasal insulin administration does not affect hepatic glucose production at systemic fasting insulin levels. *Diabetes Obes Metab* 21: 993–1000, 2019. doi:10.1111/DOM.13615.
19. **Iwen KA**, **Scherer T**, **Heni M**, **Sayk F**, **Wellnitz T**, **Machleidt F**, **Preissl H**, **Häring HU**, **Fritsche A**, **Lehnert H**, **Buettner C**, **Hallschmid M.** Intranasal insulin suppresses systemic but not subcutaneous lipolysis in healthy humans. *J Clin Endocrinol Metab* 99: E246–E251, 2014. doi:10.1210/jc.2013-3169.
20. **DeFronzo RA**, **Tobin JD**, **Andres R.** Glucose clamp technique: a method for quantifying insulin secretion and resistance. *Am J Physiol Endocrinol Physiol* 237: E214–E223, 1979. doi:10.1152/AJPENDO.1979.237.3.E214.
21. **Hamacher K**, **Coenen HH**, **Stöcklin G.** Efficient stereospecific synthesis of no-carrier-added 2-[18F]-fluoro-2-deoxy-D-glucose using aminopolyether supported nucleophilic substitution. *J Nucl Med* 27: 235–238, 1986.
22. **Patlak CS**, **Blasberg RG.** Graphical evaluation of blood-to-brain transfer constants from multiple-time uptake data. Generalizations. *J Cereb Blood Flow Metab* 5: 584–590, 1985. doi:10.1038/JCBFM.1985.87.
23. **Ishibashi K**, **Wagatsuma K**, **Ishiwata K**, **Ishii K.** Alteration of the regional cerebral glucose metabolism in healthy subjects by glucose loading. *Hum Brain Mapp* 37: 2823–2832, 2016. doi:10.1002/HBM.23210.
24. **Peltoniemi P**, **Lönnroth P**, **Laine H**, **Oikonen V**, **Tolvanen T**, **Grönroos T**, **Strindberg L**, **Knuuti J**, **Nuutila P.** Lumped constant for [(18)F]fluorodeoxyglucose in skeletal muscles of obese and nonobese humans. *Am J Physiol Endocrinol Physiol* 279: E1122–E1130, 2000. doi:10.1152/AJPENDO.2000.279.5.E1122.
25. **Iozzo P**, **Jarvisalo MJ**, **Kiss J**, **Borra R**, **Naum GA**, **Viljanen A**, **Viljanen T**, **Gastaldelli A**, **Buzzigoli E**, **Guiducci L**, **Barsotti E**, **Savunen T**, **Knuuti J**, **Haaparanta-Solin M**, **Ferrannini E**, **Nuutila P.** Quantification of liver glucose metabolism by positron emission tomography: validation study in pigs. *Gastroenterology* 132: 531–542, 2007. doi:10.1053/J.GASTRO.2006.12.040.
26. **Virtanen KA**, **Peltoniemi P**, **Marjamäki P**, **Asola M**, **Strindberg L**, **Parkkola R**, **Huupponen R**, **Knuuti J**, **Lönnroth P**, **Nuutila P.** Human adipose tissue glucose uptake determined using [(18)F]-fluoro-deoxy-glucose ([(18)F]FDG) and PET in combination with microdialysis. *Diabetologia*. 44: 2171–2179, 2001. doi:10.1007/S001250100026.
27. **Wu HM**, **Bergsneider M**, **Glenn TC**, **Yeh E**, **Hovda DA**, **Phelps ME**, **Huang SC.** Measurement of the global lumped constant for 2-Deoxy-2-[18F]fluoro-D-glucose in normal human brain using [15O] water and 2-deoxy-2-[18F]fluoro-D-glucose positron emission tomography imaging: a method with validation based on multiple methodologies. *Mol Imaging Biol* 5: 32–41, 2003. doi:10.1016/S1536-1632(02)00122-1.
28. **Karjalainen T**, **Tuisku J**, **Santavirta S**, **Kantonen T**, **Bucci M**, **Tuominen L**, **Hirvonen J**, **Hietala J**, **Rinne JO**, **Nummenmaa L.** Magia: robust automated image processing and kinetic modeling toolbox for PET neuroinformatics. *Front Neuroinform* 14: 3, 2020. doi:10.3389/FNINF.2020.00003.
29. **Iozzo P**, **Gastaldelli A**, **Järvisalo MJ**, **Kiss J**, **Borra R**, **Buzzigoli E**, **Viljanen A**, **Naum G**, **Viljanen T**, **Oikonen V**, **Knuuti J**, **Savunen T**, **Salvadori PA**, **Ferrannini E**, **Nuutila P.** 18F-FDG assessment of glucose disposal and production rates during fasting and insulin stimulation: a validation study. *J Nucl Med* 47: 1016–1022, 2006.
30. **U Din M**, **Raiko J**, **Saari T**, **Saunavaara V**, **Kudomi N**, **Solin O**, **Parkkola R**, **Nuutila P**, **Virtanen KA.** Human brown fat radiodensity indicates underlying tissue composition and systemic metabolic health. *J Clin Endocrinol Metab* 102: 2258–2267, 2017. doi:10.1210/jc.2016-2698.
31. **Soininen P**, **Kangas AJ**, **Würtz P**, **Tukiainen T**, **Tynkkynen T**, **Laatikainen R**, **Järvelin MR**, **Kähönen M**, **Lehtimäki T**, **Viikari J**, **Raitakari OT**, **Savolainen MJ**, **Ala-Korpela M.** High-throughput serum NMR metabonomics for cost-effective holistic studies on systemic metabolism. *Analyst* 134: 1781–1785, 2009. doi:10.1039/B910205A.
32. **Sanguinetti E**, **Guzzardi MA**, **Panetta D**, **Tripodi M**, **De Sena V**, **Quaglierini M**, **Burchielli S**, **Salvadori PA**, **Iozzo P.** Combined effect of fatty diet and cognitive decline on brain metabolism, food intake, body weight, and counteraction by intranasal insulin therapy in 3×Tg mice. *Front Cell Neurosci* 13: 188, 2019. doi:10.3389/FNCEL.2019.00188.
33. **Kamei N**, **Shingaki T**, **Kanayama Y**, **Tanaka M**, **Zochi R**, **Hasegawa K**, **Watanabe Y**, **Takeda-Morishita M.** Visualization and quantitative assessment of the brain distribution of insulin through nose-to-brain delivery based on the cell-penetrating peptide noncovalent strategy. *Mol Pharm* 13: 1004–1011, 2016. doi:10.1021/acs.molpharmaceut.5b00854.
34. **Hirvonen J**, **Virtanen KA**, **Nummenmaa L**, **Hannukainen JC**, **Honka MJ**, **Bucci M**, **Nesterov SV**, **Parkkola R**, **Rinne J**, **Iozzo P**, **Nuutila P.** Effects of insulin on brain glucose metabolism in impaired glucose tolerance. *Diabetes* 60: 443–447, 2011. doi:10.2337/DB10-0940.
35. **Bingham EM**, **Hopkins D**, **Smith D**, **Pernet A**, **Hallett W**, **Reed L**, **Marsden PK**, **Amiel SA.** The role of insulin in human brain glucose metabolism: an 18fluoro-deoxyglucose positron emission tomography study. *Diabetes* 51: 3384–3390, 2002. doi:10.2337/DIABETES.51.12.3384.
36. **Díaz-García CM**, **Mongeon R**, **Lahmann C**, **Koveal D**, **Zucker H**, **Yellen G.** Neuronal stimulation triggers neuronal glycolysis and not lactate uptake. *Cell Metab* 26: 361–374.e4, 2017. doi:10.1016/J.CMET.2017.06.021.
37. **Dienel GA**, **Wang RY**, **Cruz NF.** Generalized sensory stimulation of conscious rats increases labeling of oxidative pathways of glucose metabolism when the brain glucose-oxygen uptake ratio rises. *J Cereb Blood Flow Metab* 22: 1490–1502, 2002. doi:10.1097/01.WCB.0000034363.37277.89.
38. **Benomar Y**, **Naour N**, **Aubourg A**, **Bailleux V**, **Gertler A**, **Djiane J**, **Guerre-Millo M**, **Taouis M.** Insulin and leptin induce Glut4 plasma membrane translocation and glucose uptake in a human neuronal cell line by a phosphatidylinositol 3-kinase- dependent mechanism. *Endocrinology* 147: 2550–2556, 2006. doi:10.1210/EN.2005-1464.
39. **Reno CM**, **Puente EC**, **Sheng Z**, **Daphna-Iken D**, **Bree AJ**, **Routh VH**, **Kahn BB**, **Fisher SJ.** Brain GLUT4 knockout mice have impaired glucose tolerance, decreased insulin sensitivity, and impaired hypoglycemic counterregulation. *Diabetes* 66: 587–597, 2017. doi:10.2337/DB16-0917.
40. **Heni M**, **Hennige AM**, **Peter A**, **Siegel-Axel D**, **Ordelheide AM**, **Krebs N**, **Machicao F**, **Fritsche A**, **Häring HU**, **Staiger H.** Insulin promotes glycogen storage and cell proliferation in primary human astrocytes. *PLoS One* 6: e21594, 2011. doi:10.1371/JOURNAL.PONE.0021594.
41. **Hasselbalch SG**, **Knudsen GM**, **Videbaek C**, **Pinborg LH**, **Schmidt JF**, **Holm S**, **Paulson OB.** No effect of insulin on glucose blood-brain barrier transport and cerebral metabolism in humans. *Diabetes* 48: 1915–1921, 1999. doi:10.2337/diabetes.48.10.1915.
42. **Jauch-Chara K**, **Friedrich A**, **Rezmer M**, **Melchert UH**, **Scholand-Engler HG**, **Hallschmid M**, **Oltmanns KM.** Intranasal insulin suppresses

food intake via enhancement of brain energy levels in humans. *Diabetes* 61: 2261–2268, 2012. doi:10.2337/db12-0025.

43. **Kullmann S**, **Valenta V**, **Wagner R**, **Tschritter O**, **Machann J**, **Häring HU**, **Preissl H**, **Fritsche A**, **Heni M.** Brain insulin sensitivity is linked to adiposity and body fat distribution. *Nat Commun* 11: 1841, 2020. doi:10.1038/s41467-020-15686-y.
44. **Rebelos E**, **Nummenmaa L**, **Dadson P**, **Latva-Rasku A**, **Nuutila P.** Brain insulin sensitivity is linked to body fat distribution—the positron emission tomography perspective. *Eur J Nucl Med Mol Imaging* 48: 966–968, 2021. doi:10.1007/s00259-020-05064-7.
45. **Anand SS**, **Friedrich MG**, **Lee DS**, **Awadalla P**, **Després JP**, **Desai D**, **de Souza RJ**, **Dummer T**, **Parraga G**, **Larose E**, **Lear SA**, **Teo KK**, **Poirier P**, **Schulze KM**, **Szczesniak D**, **Tardif JC**, **Vena J**, **Zatonska K**, **Yusuf S**, **Smith EE**; **Canadian Alliance of Healthy Hearts and Minds (CAHHM) and the Prospective Urban and Rural Epidemiological (PURE) Study Investigators.** Evaluation of adiposity and cognitive function in adults. *JAMA Netw Open* 5: e2146324, 2022. doi:10.1001/jamanetworkopen.2021.46324.
46. **Huang X**, **Wang YJ**, **Xiang Y.** Bidirectional communication between brain and visceral white adipose tissue: its potential impact on Alzheimer's disease. *EBioMedicine* 84: 104263, 2022. doi:10.1016/j.ebiom.2022.104263.
47. **Esterson YB**, **Carey M**, **Boucai L**, **Goyal A**, **Raghavan P**, **Zhang K**, **Mehta D**, **Feng D**, **Wu L**, **Kehlenbrink S**, **Koppaka S**, **Kishore P**, **Hawkins M.** Central regulation of glucose production may be impaired in type 2 diabetes. *Diabetes* 65: 2569–2579, 2016. doi:10.2337/DB15-1465.
48. **Orava J**, **Nuutila P**, **Lidell ME**, **Oikonen V**, **Noponen T**, **Viljanen T**, **Scheinin M**, **Taittonen M**, **Niemi T**, **Enerbäck S**, **Virtanen KA.** Different metabolic responses of human brown adipose tissue to activation by cold and insulin. *Cell Metab* 14: 272–279, 2011. doi:10.1016/j.cmet.2011.06.012.
49. **Morrison SF**, **Madden CJ**, **Tupone D.** Central neural regulation of brown adipose tissue thermogenesis and energy expenditure. *Cell Metab* 19: 741–756, 2014. doi:10.1016/j.cmet.2014.02.007.
50. **Benedict C**, **Brede S**, **Schiöth HB**, **Lehnert H**, **Schultes B**, **Born J**, **Hallschmid M.** Intranasal insulin enhances postprandial thermogenesis and lowers postprandial serum insulin levels in healthy men. *Diabetes* 60: 114–118, 2011. doi:10.2337/DB10-0329.
51. **Xiao C**, **Dash S**, **Stahel P**, **Lewis GF.** Effects of intranasal insulin on triglyceride-rich lipoprotein particle production in healthy men. *Arterioscler Thromb Vasc Biol* 37: 1776–1781, 2017. doi:10.1161/ATVBAHA.117.309705.
52. **Xiao C**, **Dash S**, **Stahel P**, **Lewis GF.** Effects of intranasal insulin on endogenous glucose production in insulin-resistant men. *Diabetes Obes Metab* 20: 1751–1754, 2018. doi:10.1111/DOM.13289.
53. **Wagner L**, **Veit R**, **Fritsche L**, **Häring HU**, **Fritsche A**, **Birkenfeld AL**, **Heni M**, **Preissl H**, **Kullmann S.** Sex differences in central insulin action: effect of intranasal insulin on neural food cue reactivity in adults with normal weight and overweight. *Int J Obes (Lond)* 46: 1662–1670, 2022. doi:10.1038/s41366-022-01167-3.
54. **Hummel J**, **Benkendorff C**, **Fritsche L**, **Prystupa K**, **Vosseler A**, **Gancheva S**, **Trenkamp S**, **Birkenfeld AL**, **Preissl H**, **Roden M**, **Häring HU**, **Fritsche A**, **Peter A**, **Wagner R**, **Kullmann S**, **Heni M.** Brain insulin action on peripheral insulin sensitivity in women depends on menstrual cycle phase. *Nat Metab* 5: 1475–1482, 2023. doi:10.1038/s42255-023-00869-w.